

Constructing the Molecular Tree of Life using Assembly Theory and Mass Spectrometry

Amit Kahana^{1†}, Alasdair MacLeod^{1†}, Hessam Mehr^{1†}, Abhishek Sharma¹, Emma Carrick¹, Michael Jirasek¹, Sara Walker^{2,3} and Leroy Cronin^{1*}

¹School of Chemistry, University of Glasgow, Glasgow, G12 8QQ, UK.

²BEYOND Center for Fundamental Concepts in Science, Arizona State University, Tempe, AZ, USA

³School of Earth and Space Exploration, Arizona State University, Tempe, AZ, USA

*Email: Lee.Cronin@glasgow.ac.uk †These authors contributed equally.

The connected nature of all life on earth, dating back to the last universal common ancestor (LUCA), has been explored using knowledge of taxonomy and biochemistry, with significant insights enabled by molecular sequence data. However, in many cases reliable sequence data is not available or scarce. A molecular approach that goes beyond sequence information could allow investigating the molecular evolution of, and the relationship between, living systems in a more universal way. Here we demonstrate the first biochemistry-agnostic approach to map evolutionary relationships at the molecular scale, allowing the construction of phylogenetic models using mass spectrometry (MS) and Assembly Theory (AT) without elucidating molecular identities. AT allows us to estimate the complexity of molecules by deducing the amount of shared information stored within them when . By examining 74 samples from a diverse range of biotic and abiotic sources, we used tandem MS data to detect 24102 analytes (9262 unique) and 59518 molecular fragments (6755 unique). Using this MS dataset, together with AT, we were able to infer the joint assembly spaces (JAS) of samples from molecular analytes. We show how JAS allows agnostic annotation of samples without fingerprinting exact analyte identities, facilitating accurate determination of their biogenicity and taxonomical grouping. Furthermore, we developed an AT-based framework to construct a biochemistry-agnostic phylogenetic tree which is consistent with genome-based models and outperforms other similarity-based algorithms. Finally, we were able to use AT to track colony lineages of a single bacterial species based on phenotypic variation in their molecular composition with high accuracy, which would be challenging to track with genomic data. Our results demonstrate how AT can expand causal molecular inference to non-sequence information without requiring exact molecular identities, thereby opening the possibility to study previously inaccessible biological domains.

Mapping phylogenetic relationships among organisms is a fundamental objective in the study of evolution. Early taxonomic classifications were often pragmatic, focusing on aspects such as medicinal properties of plants or broad morphological groupings of animals¹. These early efforts in categorization, based on observable similarities and shared characteristics, established the need for a unified approach. The 18th century thus saw the introduction of more standardized hierarchical classification systems², which provided a foundation for systematic taxonomy. The 19th century brought significant advancements to this emerging evolutionary paradigm, with the recognition that different taxonomic groups might share common ancestry through evolutionary processes³. This concept, supported by comparative phenotypic analysis across species, led to the development of phylogenetics. These developments culminated in the modern conception of the “tree of life”, a unifying model capturing evolutionary relationships across biological forms⁴⁻⁶.

Though the core concepts of evolution underlying the idea of the tree of life have not changed, the tree itself has been refined and expanded through advances in genetics, molecular biology, and computational methods, providing increasingly detailed and accurate representations of evolutionary history across life on Earth. The application of molecular approaches to tree construction has only been accelerated by the introduction of affordable and high-throughput sequencing methods over the last several decades. These have been successful enough to place sequence information as the forefront, and often sole, source of molecular information used to link terrestrial lifeforms across time. Indeed, the wealth of biochemical knowledge accumulated over the years has empowered the scientific community to develop sophisticated algorithms for exploring evolutionary relationships with sequence data, which have significantly enhanced our understanding of the history and evolution of life on Earth⁵⁻⁸.

However, relying on gene sequences as the sole source of molecular information for inferring evolutionary relationships comes with substantial limitations that have been difficult to overcome. Fast evolving entities like viruses often defy being rooted in an evolutionary tree⁹. Though genomics have allowed detection of many unculturable microorganisms, their sequenced data is often sparse,

inconsistent and functionally unannotated, leaving much of Earth's extant biodiversity unmapped^{10–12}. Furthermore, the protobiological evolving entities that may have preceded the last universal common ancestor plausibly did not contain genomic information^{13,14}, meaning that even as we expect molecular fossils to be relics from a phase of evolution preceding the modern genome¹⁵, it is not possible to study these very deep evolutionary processes below the root of the current tree of life based on genomically-derived information alone.

Chemotaxonomy, the process of classifying and identifying organisms based on the similarities and differences in their biochemical compositions, has progressed to provide excellent examples where chemical analyses of biological samples assist in their classification^{16–20}. Metabolomic data has also been used as a means to detect and quantify the concentration of predefined biomarkers²⁰, especially large polymeric metabolites²¹. The models generated on the basis of quantitative metabolomic data have been used to research families of plants²², fungi²³ and insects²², as well as mammalian and human microbiomes^{20,24} among others. However, this approach is constrained by the availability and the quality of reference molecular-spectrum libraries, and therefore often involves low metabolome coverage, oblivious to the many other molecules whose biological roles are not readily discernible and catalogued^{20,21,25,26}. In so, these approaches are not agnostic and thereby remain limited to biochemistry that is already known – currently, no molecular methods allow exploration of living forms whose biochemistry is not previously explicated and experimentally identifiable.

We hypothesize that Assembly Theory (AT) in conjunction with mass spectrometry (MS) measurements could be used to go beyond methods requiring prior fingerprinting of molecular species, allowing mapping relationships of evolving systems where sequence data is sparse or non-existent²⁷. According to AT, every molecule has an inherent complexity (Molecular Assembly, MA) corresponding to the shortest construction pathway of its molecular graph. Central to AT is the concept of an assembly space, composed of a molecule's precursors along its construction pathway, where each fragment is recursively built up from simpler building blocks. The smallest possible cardinality of the assembly space is indicated by the target molecule's MA, quantifying the minimal

number of constraints necessary for the construction of the molecule. It has been demonstrated that this metric can be experimentally inferred using mass spectrometry and other analytical techniques²⁸, and previous work empirically verified that organic molecules with high MA values are indicative of life, presenting MA as a genome-agnostic method for life detection²⁷.

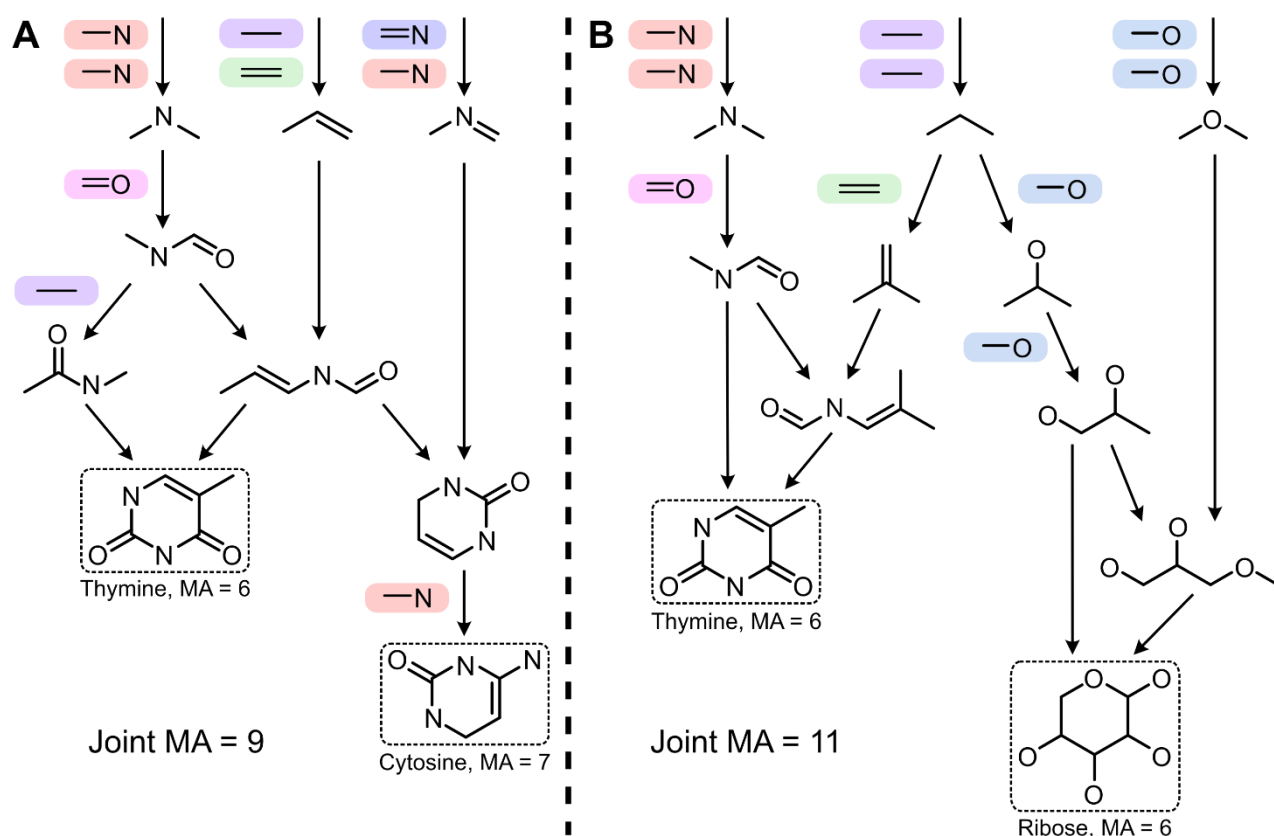


Figure 1. Joint Assembly Spaces of molecules. **A)** The joint assembly space (JAS) of Thymine and Cytosine, consisting of their combined assembly pathways to give the shortest sequence of joining operations for their simultaneous construction. **B)** The JAS of Thymine and Ribose. The individual MAs of Thymine, Cytosine and Ribose are 6, 7 and 6 respectively. Noticeably, Thymine is more similar to Cytosine, with a Joint MA of 9, compared to Ribose, with a Joint MA of 11. This can be seen in the displayed assembly pathways, as Thymine and Cytosine share more sub-objects than Thymine and Ribose.

The concept of assembly space can be generalized to apply to a set of distinct molecules, more befitting biological samples comprising molecular networks, where the simultaneous construction pathway for the entire set of molecules together is called a Joint Assembly Space (JAS) (**Figure 1**). The shortest pathway in a JAS represents the minimal set of constraints required to construct a given ensemble of molecules simultaneously²⁹, and the number of steps along this pathway is termed Joint Molecular Assembly (Joint MA). The JAS is comprised of the target objects measured at a single

point in time, and of the contingent objects along their assembly pathways. Within the framework of a generalized AT, these respectively correspond to the Assembly Observed, the space of all objects that are observationally confirmed, and the Assembly Contingent, the space of all contingent sub-objects generated from assembly pathways that are governed by historical contingency³⁰. The formulation of a JAS can be used as a tool to reveal contingent relationships between individual molecules or entire chemical systems, particularly important for cases where the exact chemical reaction pathways are very complex or the temporal formation histories of molecules are unknown, as these are unnecessary information for the JAS. Moreover, the JAS does not have explicit knowledge of geological time; however for a set of complex molecules it does encode the underlying causal relationships that have a necessary temporal ordering for the production of a set of molecules, providing causal constraints on any process that might co-construct those molecules, including evolutionary processes.

Incorporating complexity considerations into molecular analyses could provide further insights into the informational architecture that governs biological life-forms³⁰. A biological cell is a self-constructing molecular network, which stays largely at compositional homeostasis (composome, a quasi-stationary state)^{14,31} through intricate molecular interactions, an evident result of selection. Evolution facilitates the transformation of these networks over time, allowing exploration of new molecular compositions (Assembly Observed), and their underlying assembly spaces (Assembly Contingent) that lead to molecular and functional novelty³⁰. It has been shown that higher levels in the informational organization of the cell, such as the phenome and the genome, can be elucidated with a bottom-up inference based on idiosyncratic signatures in the compositional metabolome^{25,32}, see **Figure 2A**. In this light, the metabolome may be regarded as an expansive informational arena describing the historical contingency of the cell³³. We therefore hypothesize that genome-agnostic molecular information, coupled with AT, may allow the inference of evolutionary trajectories, manifesting in the contingent transformation through time of the assembly spaces of molecular networks from common ancestors to current day species (**Figure 2B**).

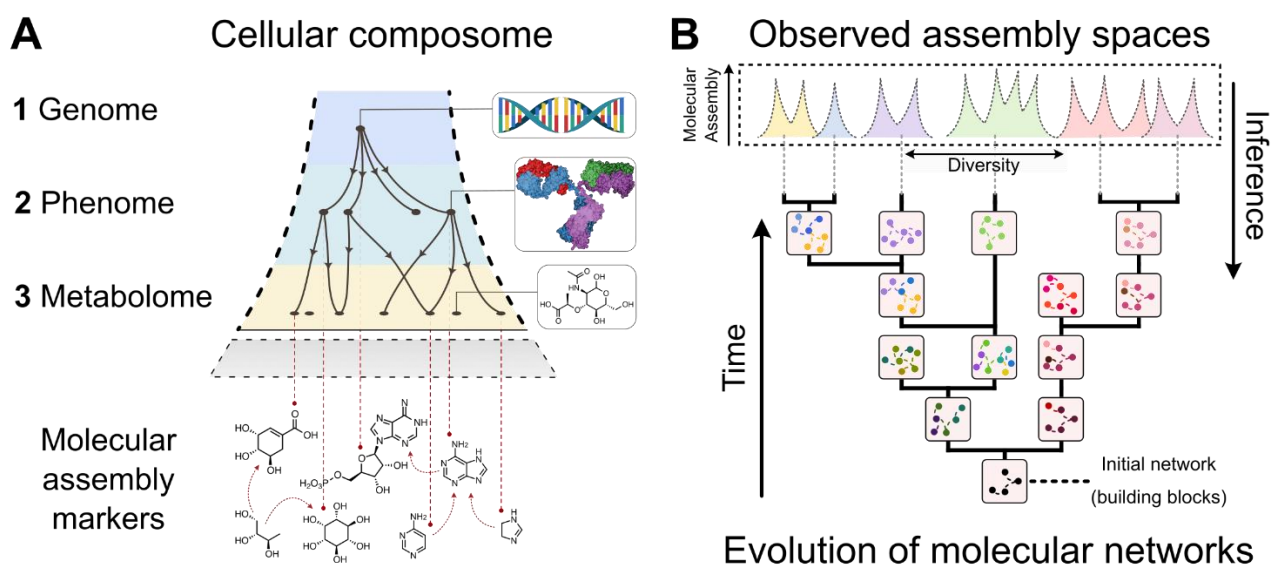


Figure 2. Assembly spaces of biological systems undergoing evolution. **A)** The cellular composome and its informational architecture. The flow of information is portrayed, from the genome to the phenome (e.g. proteins and ribozymes) and the metabolome. Observable analytes from these levels serve as molecular assembly markers, which give information about the assembly space underlying the cellular composome, and which can inform about the unique identity and state of the cell. **B)** An assembly representation of evolution as a tree of molecular networks, from an initial network composed of an assortment of building blocks towards more defined and complex organismal networks. The molecular networks evolve over time and become more distinctly associated with recent clades. The observed assembly spaces of molecular networks are shown at the top, defined by the diversity and complexity of their molecular structures and used for phylogenetic inference. Colors indicate association to specific phylogenetic grouping, and their idiosyncratic traces through their inferred evolutionary past.

In this study, we propose a generalised method of inferring the JAS of the cellular composome and demonstrate that it applies not only to life detection (as in prior work) but also to life classification, reflecting the causal relationships between species as complex chemical networks. We demonstrate the utility of this approach both over longer term evolutionary trajectories, and short-term phenotypic trajectories leading to divergence in populations where no detectable genomic evolution has yet sufficiently occurred. Using AT, we were able to generate a phylogenetic tree of life - using only mass spectrometry data of small metabolites - that conforms with current biological knowledge, offering a comparable alternative to other phylogenetic methods that does not require prior molecular fingerprinting, see **Figure 3**. We further applied our AT methodology to deduce the genealogy of recursive culturing of bacterial colonies, demonstrating its ability to reveal very short-term historical contingency among low-genomic-variation samples of the same species. Thus our study illustrates that the distinct molecular networks of biological cells carry information about their long-term

evolutionary past as well as short term phenotypic history, which can be deciphered and employed as a universal apparatus for life detection and the classification of life along diverging lineages on short and long timescales.

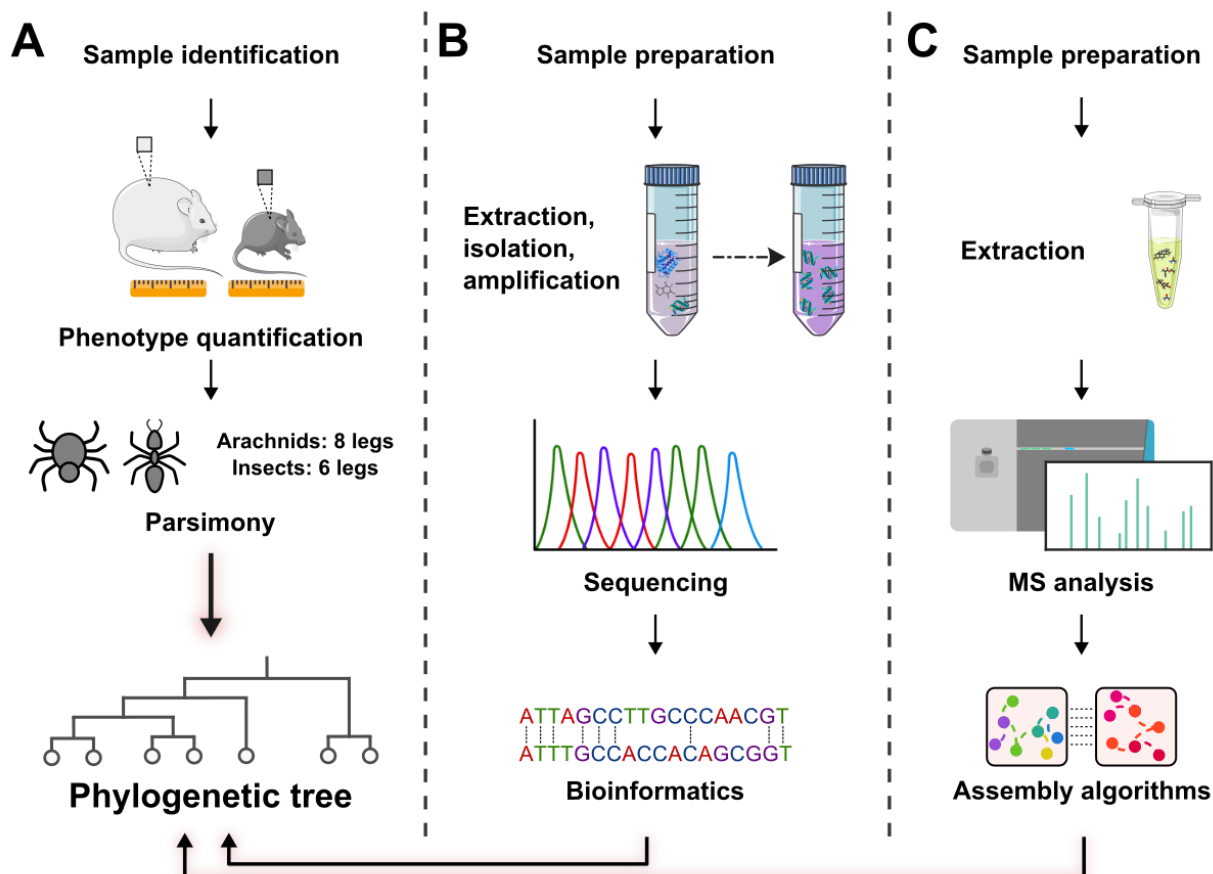


Figure 3. Comparison between different phylogenetic inference methods resulting in a phylogenetic tree. **A)** Differentiation according to morphology. **B)** Differentiation according to sequencing information. **C)** Differentiation according to assembly spaces (this work).

Results and Discussion

Fingerprinting idiosyncratic MS-derived profiles of samples

The analytical process allowed us to gather information about the analytes residing in the organismal samples. Even though the analytes were not structurally elucidated, we hypothesized that non-targeted MS¹ and MS² information could be sufficient for species classification. Data exploration showed that this is particularly true for differentiating between living and non-living samples – analysis of inorganic samples revealed distinctly less intense peaks (**Figure 4A**) and fewer analytes

altogether (**Figure 4B**). We approached each set of analytes as an fingerprint of a sample's molecular network, demonstrating unique idiosyncratic features that allow its potential classification within a larger group or clade (**Figure 4C**).

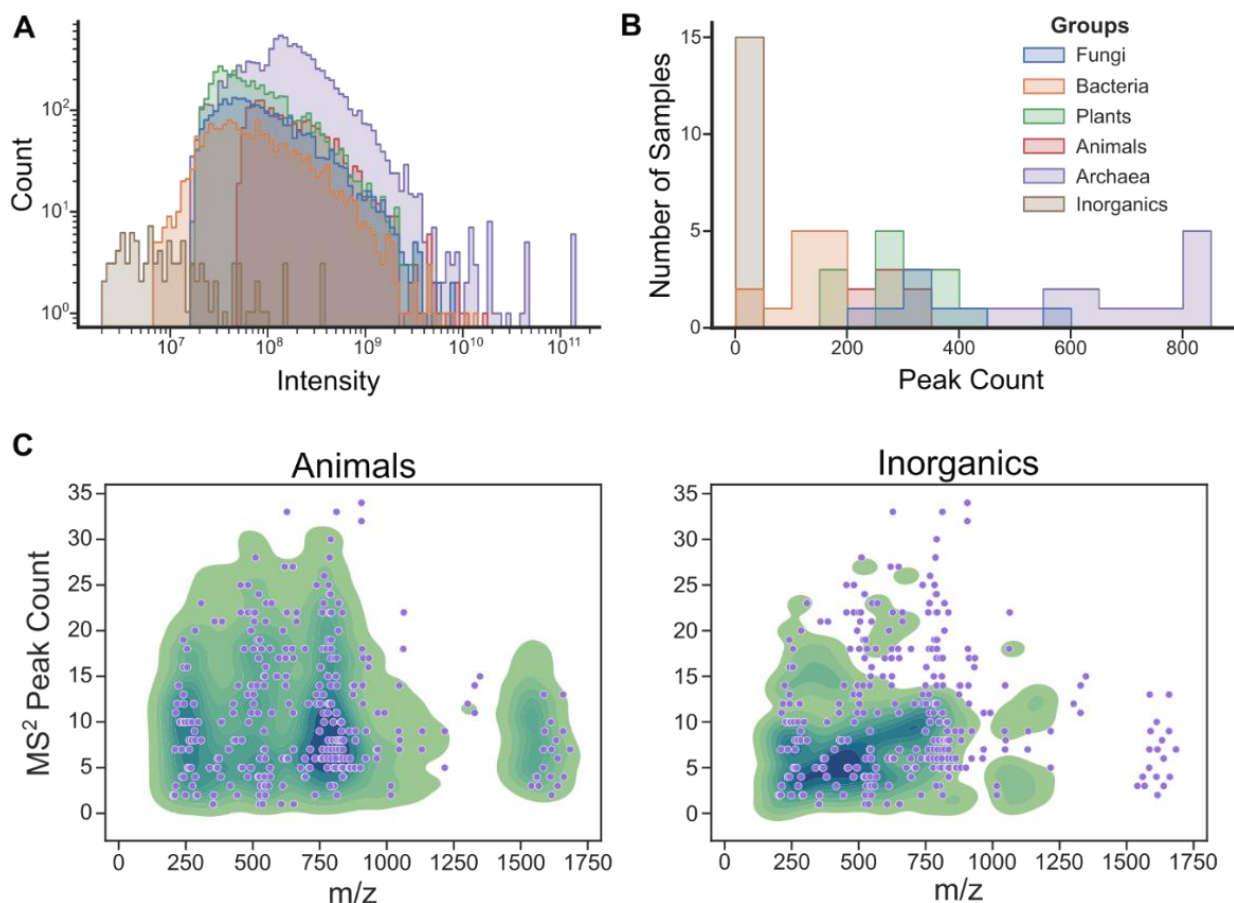


Figure 4. Fingerprinting molecular networks. **A)** Histograms of the intensity of peaks detected for all samples within the labeled groups. **B)** Histograms of the number of peaks detected for samples within each labeled group. **C)** Analytes from a Cod sample (purple) layed over Kernel Density Estimate (KDE) maps of the Animals and Inorganics (minerals) groups (green), according to the m/z and number of MS^2 peaks of their associated analytes. The KDE bandwidth estimation was conducted with a scaling factor of 0.55. Scatterplots and KDE maps for all samples and groups can be found in the SI section 6.

To validate our experimental approach, we tried to match the detected analytes from the *E. coli* sample to known metabolites with reference or predicted spectra (see methods). Most detected molecules do not map to known or predicted spectra of *E. coli* metabolites, possibly due to algorithmic limitations. Alternatively, they may belong to an underground metabolism, encompassing reactions that are not genomically encoded and thus not readily investigated and recorded²⁶. Nevertheless, the results reveal

several universal biomolecules with high certainty (such as nucleobases, amino acids, sugars, and organic cofactors) as well as more specific bacterial lipids with lesser certainty (see SI section 7). This reaffirms our analytical procedure is general enough for the detection of distinct analyte chemistries across a wide mass-range, allowing faithful metabolic mapping of organismal samples.

Genome-agnostic mapping of phylogenetic relations between organisms

The experimental MS data of the organismal samples have significance in the generalized AT (**Figure 5A**). As stated above, the detected MS¹ analytes represent the Assembly Observed of the samples, since these are direct measurements of real molecular components of the cell. The sets of MS² molecular fragments are the result of empirical deconstruction of their detected precursor analytes. Thereby they represent the extended Assembly Contingent, since they sample the space which comprise all possible pathways to assemble the sets of detected molecules. By sampling the extended Assembly Contingent of the organismal samples, we can construct possible assembly pathways of different lengths, with the fragments acting as contingent objects within the space. The space of MS-based pathway construction of all molecules within an organismal sample is therefore comparable to a JAS²⁹, which refers to the combined assembly steps and substructures included in the graphical assembly process of an examined set of target objects. Deeper levels of tandem MS correspond to join operations between smaller fragments, which scale up in complexity across the MS data levels towards their original molecular precursors, emulating the JAS hierarchical structure (see **Figure 1**). This comparison is especially potent considering all metabolites and their fragments originate from the same metabolic synthetic system, an elaborate network of interconnected pathways expanding from a shared set of basic building blocks. We therefore named the MS-derived construction space a Joint Fragment Assembly Space and set to investigate its causal relationships using AT analytical tools.

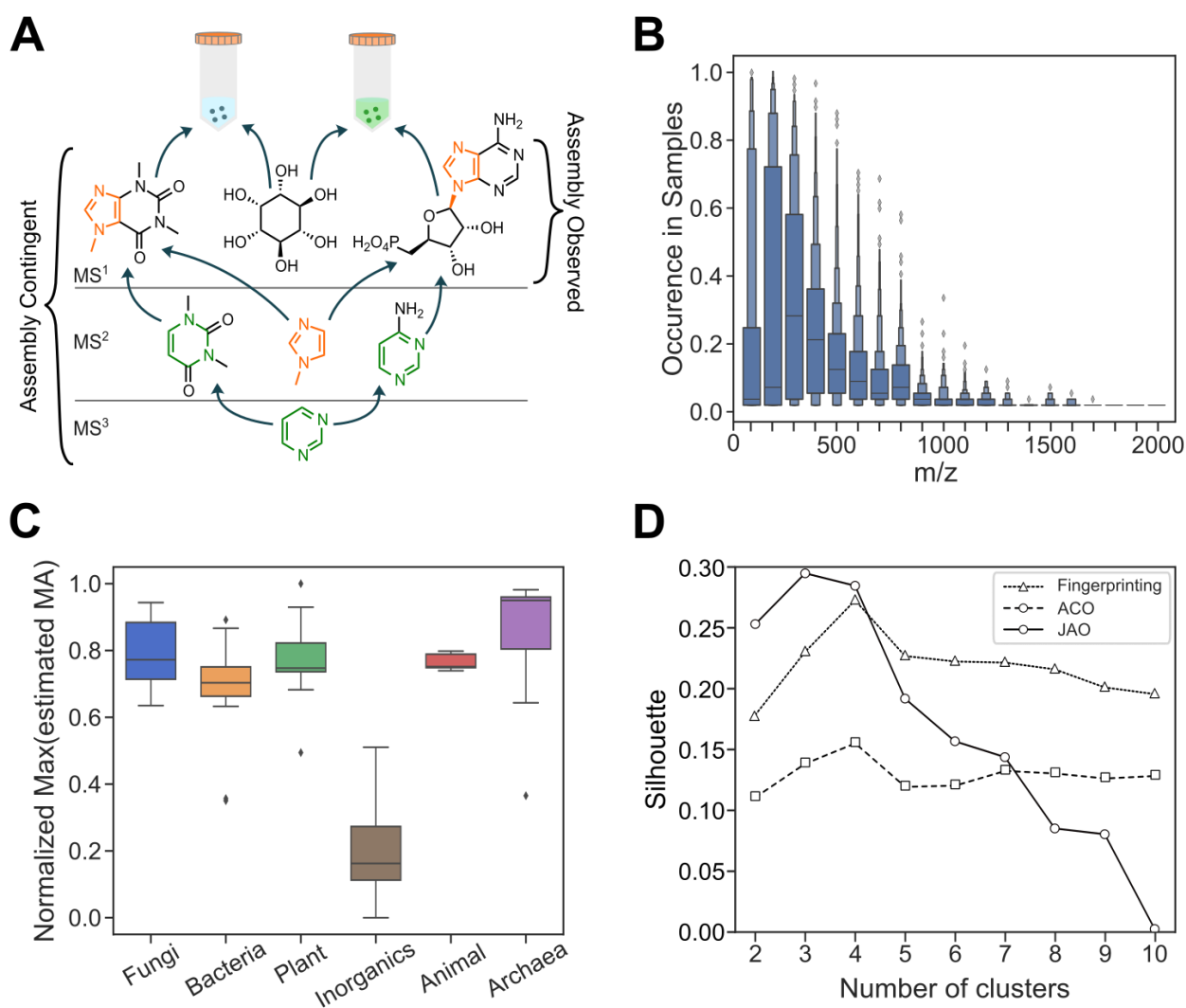


Figure 5. Assembly-based analyses and classification of composite MS information. **A)** Schematic representation of the MS-based Joint Fragment Assembly Space of two multimolecular samples with shared metabolites. The scheme represents an inferred pathway across the MS levels, an emulation of the results obtained with the Recursive MA algorithm. **B)** Boxenplots of all MS² fragments observed in the analysed samples, showing their m/z and their occurrence in the samples dataset. Each box represents a bin of 100 Da. **C)** Boxplot of the maximal estimated MA of each sample for each group, calculated with Recursive MA and normalized across the set. **D)** Spectral clustering over samples using the assembly-based phylogenetic methods (Fingerprinting, ACO and JAO) for cladal domain classification, presenting Silhouette scores for each number of clusters in the model. The Silhouette score indicates how similar the objects within the clusters are to each other compared to objects in other clusters, with high values indicating better clustering scheme.

To uncover the underlying cladistic architecture of the samples, we developed a numeric model based on the Recursive MA algorithm²⁸ that operates on hierarchical tandem MS data to constrain and estimate MA values for target molecules. By employing the Recursive MA algorithm, we generated Joint Fragment Assembly Spaces for each individual sample in our dataset, recursively constructing

their composite analytes from tandem MS data and pooling together their shortest detected construction pathways (**Figure 5A**). We then calculated an approximated Joint MA values for discrete organismal samples, describing the estimated level of complexity of their molecular ensemble (see SI section 8). By comparing the approximated Joint MA of individual and groups of samples, we were able to estimate the Joint Assembly Overlap (JAO) of the samples examined (see methods). This metric describes the relatedness of species in the dataset based on the similarity of the shortest construction pathways calculated for their MS-based JAS (see methods). This analysis does not rely on any prior molecular information of the detected analytes, thus enabling agnostic phylogenetic inference. The interrelated evolutionary trajectories of species from shared ancestors explain why there is a degree of shared MS² fragments among different molecules within and across samples, as it is unlikely that samples will possess similar molecular species by chance given the enormity of chemical space³⁴. Indeed, a larger number of mostly lower-mass fragments occur in multiple samples, with the probability of shared fragments among samples diminishing at higher fragment masses (**Figure 5B**). This illustrates the prevalence of shared objects in the Assembly Contingent of organismal samples, supporting the applicability of JAS for elucidating evolutionary trajectories.

Biogenicity determination and cladal domain classification with assembly spaces

To investigate the capacity of AT to correctly discriminate between defined groups of samples, we employed it for two discrete tasks. First, we attempted to distinguish between biological and non-biological samples. We used two classification methods: a supervised leave-one-out cross validation approach, and an unsupervised spectral clustering approach (see methods). We compared the JAO metric with two simpler metrics based on AT. The first is an overlap of the detected MS¹ analytes, a fingerprinting approach of biomarkers which span the Assembly Observed of the samples, using a heuristic Otsuka-Ochiai coefficient (OOC) akin to cosine similarity³⁵. The second metric is the Assembly Contingent Overlap (ACO), a mass-weighted OOC overlap of the MS¹ and MS² data of the samples which span their measured Assembly Contingent (see methods). ACO is pathways-

agnostic as it spans possible contingent objects without join operations, fundamentally different to the JAO approach. All metrics presented comparably successful prediction results, easily determining the biogenicity of samples in both targeted and non-targeted classification methods with very few errors (see SI section 8). Notably, blind biogenicity determination can be reliably achieved beyond relational clustering by looking at the MA of molecules detected in samples²⁷, and this can be clearly seen in our dataset (**Figure 5C**).

Further, we tested whether we can correctly annotate biological samples as belonging to different predefined cladal domains, including Animalia, Archaea, Bacteria, Fungi and Plantae. In the supervised cross-validation approach, all metrics portrayed excellent classifications for very few errors. In the unsupervised clustering method, both the fingerprinting and ACO approaches showed no change in the clustering accuracy with varying number of clusters, with the former outperforming the latter. This may be indicative that the clusters are very molecularly distinct, which is captured better by Assembly Observed than Assembly Contingent (**Figure 5D**). The JAO metric performed marginally better with few clusters, capturing a cohesive partition of samples into major domains. The grouping of samples alongside the clustering operation depicted very logical decision-making that follows evolutionary trajectories, where taxonomical groups separate according to their rank and chronology (see SI section 8). The overall silhouette values were generally low, which is appropriate considering the hierarchical nature of the data. This may be the reason why the JAO metric shows a decline trend in the silhouette plot, contrary to the other two metrics (**Figure 5D**). Given these results, it appears that the more heuristic approaches (fingerprinting and ACO) approximate the JAS inference (JAO), which captures better the causal hierarchical structure of the dataset.

Agnostic tree of life inference using assembly theory

Contrary to the cladal domain classifier, phylogenetic inference does not rely on database comparison or predefined group annotation. It is often performed without *a priori* taxonomical information, and requires more complete datasets, as it aspires to infer evolutionary trajectories across time, and their

interconnectedness. Using our phylogenetic pipeline (**Figure 6A**), we generated agnostic tree of life models based on MS information elucidated via AT. The trees generated by the JAO method generally display rational phylogenetic clustering, closely reflecting evolutionary trends that appear in genome-based phylogenetic studies, most importantly the cohesiveness and consolidation order of general cladal domains (**Figure 6B**). In comparison, while a tree produced by the fingerprinting approach gave a similar result, one generated using the ACO method did not adequately capture known and deducible evolutionary trends – clustering choices reveal limited success in outlining cohesive cladal domains (see SI). It appears that the detected analytes (Assembly Observed) are sufficient to differentiate between samples, and that fragment information (Assembly Contingent) adds too much interference to the model. Nonetheless, the fact that JAO performs so well suggests that a ground truth assembly-based approach is essential for an accurate MS-based cladistic configuration.

Closer examination of the resultant tree of life model reveals more reasonable clustering details (**Figure 7A**). Samples that belong to the same species are closely positioned together (see SI), and there is logic to the clustering at the lower levels, such as the cohesive clustering of all *Staphylococci* species, and the partitioning of halophiles and acidophiles in the archaea domain. Furthermore, there are some interesting cladistic choices that could be a result of our analytical procedure and particular choice of samples. For instance, nuts and seeds are associated closely, possibly reflecting their unique metabolic constitutions which may not be representative of other plant tissue. Similarly, in the animalia kingdom, land and sea animals cluster separately, though this is not far from the genomic model for this set of samples (see SI section 8). Those phenotypic mappings may be overcome by more representative sampling, and by increasing the analyte coverage of the samples, further establishing the unique identities of the molecular fingerprints necessary for classification. It may explain some of the clustering choices for samples of fewer analytes, such in the bacteria domain. However, these potential phylogenetic misclassifications are relatively minor, and reaffirm the reliability of our approach. Altogether, it appears that the agnostic tree of life produced by our

assembly-based phylogenetic model using non-targeted small metabolite information offers evolutionary insights that appear consistent with consensual biological knowledge.

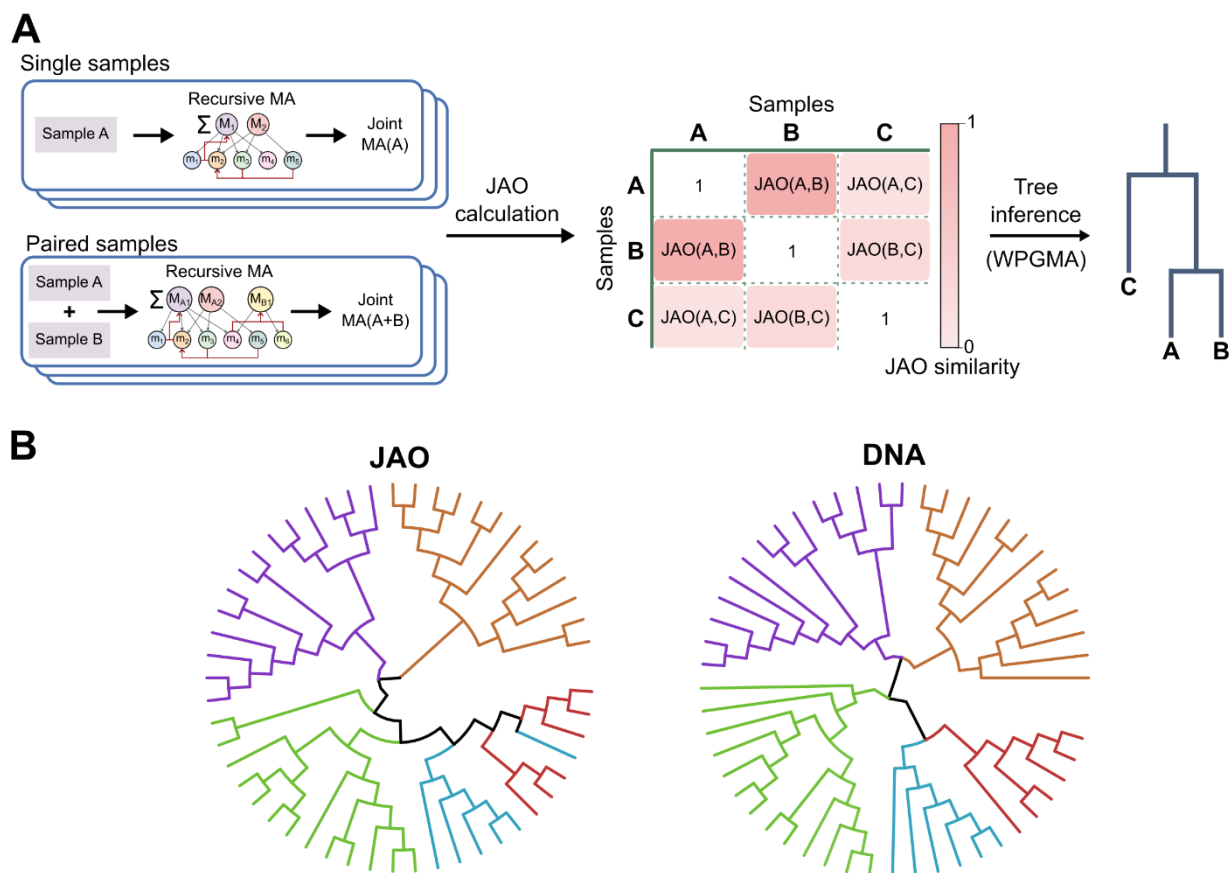


Figure 6. Phylogenetic inference using Assembly Theory. **A**) Algorithmic pipeline for the generation of a phylogenetic tree from MS data using Joint Assembly. Recursive MA is employed to calculate approximated Joint MA indices for single and paired samples, which are used in JAO calculations (see methods). The JAO matrix represents the overlap of joint assembly spaces of samples, which is then transformed into a tree through an inference algorithm (WPGMA). **B**) Comprison of the assembly-based JAO phylogenetic tree model with the consensual genome-based model. Colors refer to the predefined cladal domains, as in Figures 4, and indicate the cladal cohesiveness of the clustering. Full annotations of the trees are included in Figure 7 and SI.

Validation of assembly phylogenetics

To substantiate our tree of life model, we first inspected the data-driven decisions of our assembly-based phylogenetic algorithm. We observed that samples that are more closely clustered on the JAO tree tend to share a higher degree of high-mass fragments (**Figure 7B**). This can be gleaned from an increasing contribution of low-mass fragments, and a decreasing contribution of high-mass fragments, to the set of fragments shared across samples for more distantly related samples on the tree. This finding substantiates the model and connects it further to the fundamentals of AT, where

molecules of higher masses (which correspond to higher MAs²⁷) indicate an increased contingency in their assembly pathways, which is manifested in the tree model.

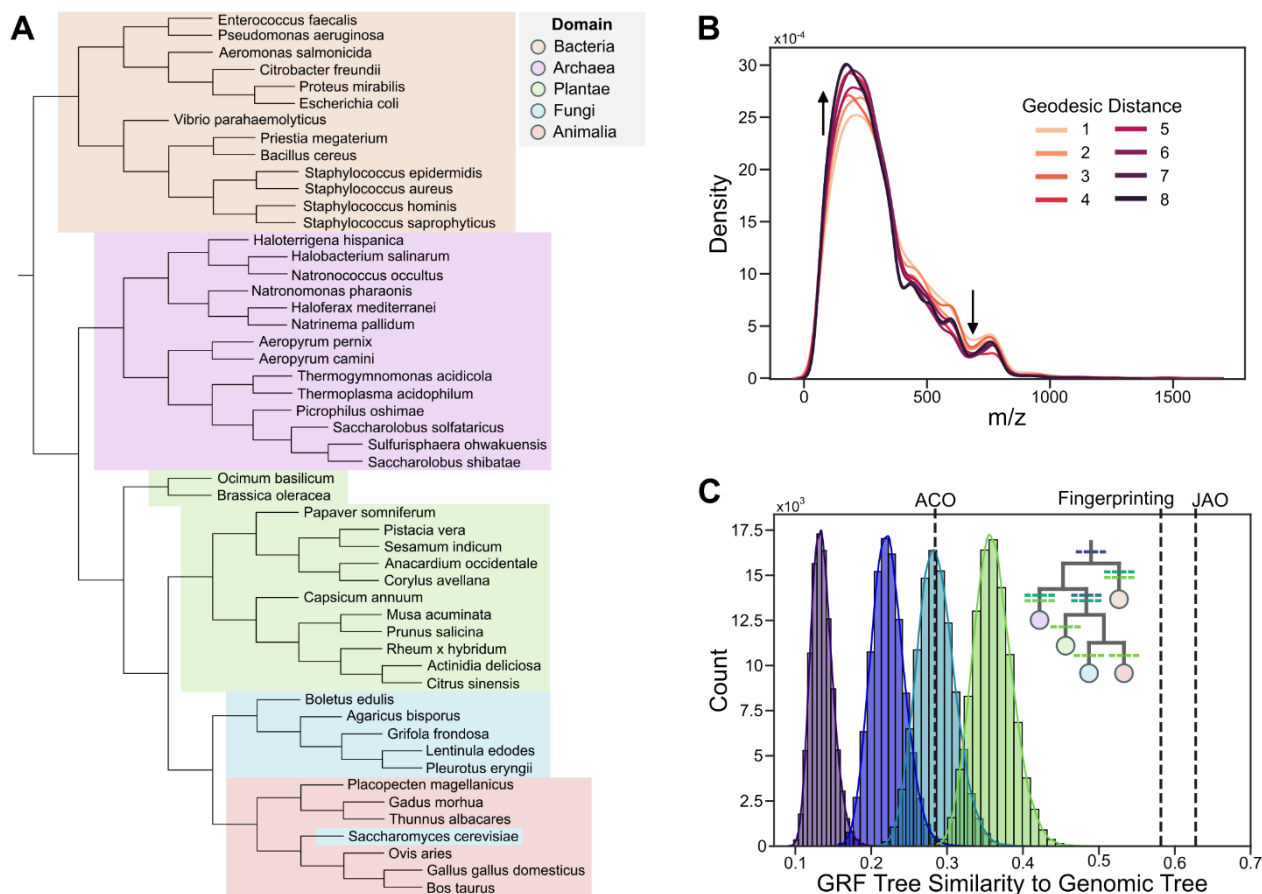


Figure 7. Assembly-based phylogenetic Tree of Life from non-targeted metabolite information. **A)** The JAO tree with species annotation. The position of samples within this tree is not pre-determined by *a priori* cladistic knowledge, such as through genomic, proteomic or metabolic information. Colours refer to cladal domains. Lengths of the branches correspond to 2 minus JAO of the clustered clades. **B)** Kernel Density Estimate (KDE) plots of the m/z values of all shared MS^2 fragments between samples of different geodesic distances in the JAO tree model. Arrows indicate the trends in the data. **C)** Histograms of randomly-generated phylogenetic trees models showing their Generalized Robinson-Foulds (GRF) similarity scores to the consensual genome-based tree model. The different distributions refer to higher degree of constraints in the randomness of the tree generation, depicted in the inset, where randomness was allowed within predefined cladal groups. Purple – completely random, blue – separating prokaryotes and eukaryotes, light blue – separating the bacterial, archaeal and eukaryotic domains, and green – separating the cladal domains of bacteria, archaea, plants, fungi and animals. Colored circles in the inset refer to the cladal groups as appeared in A. The vertical dashed lines represent the score of the assembly based tree models, which are 0.58 for the fingerprinting, 0.28 for ACO and 0.63 for JAO. T-tests of the JAO model against the randa-trees distributions all results in essentially p -value = 0.0.

Second, we compared our assembly-based trees to a consensual phylogenetic tree (generated from the TimeTree database³⁶), to examine whether our agnostic models conform with models constructed

from genomic information. We generated distributions of random trees with different levels of constraints and compared them to the genomic tree using the Generalized Robinson-Foulds (GRF) similarity³⁷ (**Figure 7C**) and the Quartet similarity (see SI) metrics as robust phylogenetic analytical metrics³⁸. The GRF similarity metric describes the common taxa among the trees, i.e. the shared sets of samples that are hierarchically clustered in both tree models. The Quartet similarity metric describes the fraction of quartets of samples that are clustered similarly between the tree models. The results of both analyses reveal that the fingerprinting and JAO assembly-based trees are substantially non-random and align well with the genomic tree with high statistical significance. In contrast, the ACO tree model presented low similarity values with the genomic tree, positioned among the random tree distributions.

Phylogenetic inference of single-species lineages

To further substantiate our MS-based phylogenetic approach, we tested it on a case where both morphological and genetic inferences would be challenging and less effective in predicting accurate phylogenetic structures. We decided on a bacterial growth system in which *E. coli* was recursively cultured and plated, absent of any exerted selection pressure, keeping genomic variation to a minimum. In each recursive cycle, an *E. coli* culture was plated and two colonies were picked from the plate and cultured separately, generating an overall tree-like experimental design comprising four bacterial generations (**Figure 8A and 8B**). In this system, the phylogenetic inference was not meant to predict the evolutionary history of distinct species, but the phenotypic trajectories of related colonies of the same species, based on their detected molecular compositions.

The analysed samples revealed a significant degree of homogeneity, as expected. We detected 2186 unique MS¹ analytes and 1925 unique MS² fragments across the eight leaf nodes in the tree, each individual sample comprising about 1400 analytes and 1300 unique fragments. The low variation across the dataset signifies a pronounced difficulty to elucidate the experimental tree structure. Indeed, a simple OOC fingerprinting approach of the detected metabolites gave an almost completely

random tree prediction at the 62nd percentile of all possible trees (**Figure 8C**). The more assembly-based metrics performed significantly better, with JAO and ACO giving tree predictions at the 96th and 99th percentiles respectively.

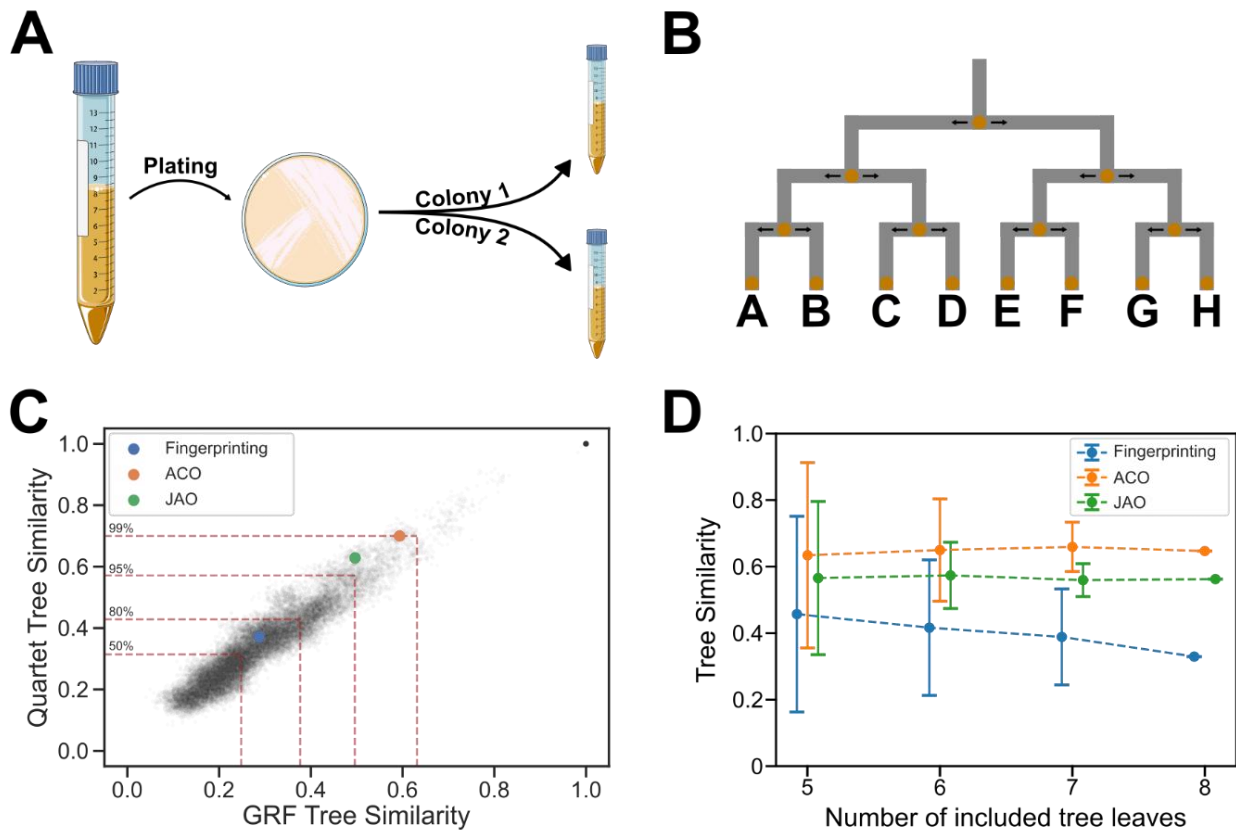


Figure 8. Deducing bacterial lineages by Assembly-based phylogenetics. **A)** A schematic representation of a recursive step in the experiment, consisting of plating a culture of *E. coli* and reculturing two picked colonies from the plate. **B)** The tree-like structure of the recursive experiment, spanning four generations of colony culturing, and resulting in eight leaf node samples indicated by bold letters. **C)** A scatterplot detailing the capacity of the phylogenetic algorithms to predict a tree that closely resembles the actual experimental tree structure, assessed by GRF and Quartet tree similarity metrics. The black dots represent every possible tree structure comprised of eight leaf nodes (135,135 trees), and their tree similarity values with normally-distributed errors for better visual dispersion. The red dashed lines represent percentiles of trees included within the encapsulated areas. **D)** A plot depicting the prediction accuracy of the phylogenetic algorithms in relation to the number of samples included in the tree. The calculations were done through an exclusion assay, in which every possible tree permutation of *n* nodes was tested, comparing the predicted tree to the actual experimental tree structure. The tree similarity used was an average of the GRF and Quartet values obtained for each prediction. Error bars represent standard deviations.

This means that only one percent of all possible tree structures are closer to the true experimental tree than the assembly tree prediction. This nontrivial prediction feat by the assembly-based metrics appears to be indifferent to the size of the dataset, whereas the accuracy of the fingerprinting approach goes down the more samples are included in the tree (**Figure 8D**). Moreover, the assembly-based

metrics seem to be more consistent and less influenced by outliers than fingerprinting, showing lower variance of prediction accuracy. These results illustrate the adeptness and reliability of assembly to correctly infer phylogenetic and causal relationships from molecular observations in highly homogenous and temporal systems that would prove challenging for previously established techniques.

Conclusions

The transformative discovery of the genome as a common underlying substrate for recording evolutionary change across biology unified the empirical investigation of all life forms on the planet and enabled the study of deep time connections between species in a quantitative, objective manner. With the advent of Assembly Theory, we now have a more general framework within which to study the causal relationships between molecular ensembles of any origin, be it biotic or abiotic. In this work we used this framework to devise a simple quantitative system for detecting and classifying living species without reference to their genetic material, or indeed any prior knowledge of their biochemistry, using a robust general analytical workflow. We presented a non-targeted genome-agnostic direct examination of molecular compositional information of living and non-living species and developed models to employ it for accurate phylogenetic inference. We were able to reliably discern the biogenicity of samples and their cladal grouping with supervised and unsupervised methodologies. We then generated phylogenetic tree of life models that closely resemble the consensual genomic tree model, all without prior genomic, proteomic or metabolic knowledge of the samples. Finally, we employed our methodology to track the genealogy of a single bacterial species, strengthening the generality and expediency of Assembly. We conclude that our agnostic assembly-based tree model can be used to map the evolution of life on earth, tracing the contingent history of molecular ensembles without depending on particular chemical or biological features. This approach has the potential to provide an efficient diagnostic tool that may complement genome-based efforts,

and should expand our understanding of life, its origin and evolution, beyond current models and definitions that are anchored in the specificity of the biological inception.

Methods

Sample preparation

A variety of animal, bacteria, fungi, plant, and inorganic samples consisting of complex analyte mixtures were prepared and analysed to garner information on molecular assembly. Animal, plant, and fungi samples were frozen immediately in a -40 °C freezer for 24 hours before freeze-drying (-48 °C, 1.8 mbar) for 48 hours. These were subsequently ground in a mortar and pestle and sieved to produce particle sizes < 0.5 mm. Bacteria samples were cultured overnight in nutrient broth, at 37 °C, then centrifuged to separate the broth supernatant from the bacteria pellet. Inorganic samples were crushed and sieved to produce particle sizes < 0.5 mm. To procure a wide range of metabolites, ultrasound-assisted extraction (UAE, 20 mins/30 °C) was employed with 10 mL of 80% methanol extraction solvent. For each sample, three sample replicates and a control were investigated. Further details of the extraction process are available in the SI section 3. Samples were analysed using HPLC-MS/MS. The comprehensive methodology for the HPLC and Orbitrap Fusion Lumos mass spectrometer are reported in the SI section 4.

MS² Optimisation

The complex nature of our unprocessed samples necessitated an adaptive analysis protocol, implemented via data-dependent MS/MS acquisition (DDA), whereby the most intense analytes from MS¹ scans are selected for MS² fragmentation³⁹. However, DDA can encounter limitations that result in the incomplete sampling of detectible analytes, such as constraints on the number of analytes available for MS/MS due to scan speed, masking of analytes by contamination and noise⁴⁰. Since it was crucial to improve the abundance and quality of MS² spectra for these overlooked analytes⁴¹, a modified DDA approach was developed whereby an initial MS experiment was conducted to obtain

a list of analytes (an inclusion list) unique to each sample, devoid of contamination and noise, before a secondary MS experiment was conducted specifically fragmenting analytes from the inclusion list. Details of the construction of the inclusion list can be found in the SI section 5. For the recursive culturing experiment of *E. coli*, we used the AcquireX automated data-acquisition procedure similar to our modified DDA procedure used for the Tree of Life samples for improved analyte detection⁴².

Tree of life modelling

Within the generalized AT, we formulated the fingerprinting method to be a simple overlap of MS¹ analytes between samples, and ACO to be an overlap of the MS¹ analytes and MS² fragments between samples weighted by their mass. We used the mass-weights for ACO as a first-approximation of their MAs²⁸, which more closely span the Assembly Contingent and improve classification. To achieve that, we employed the Otsuka–Ochiai coefficient (OOC)³⁵, a variation of a cosine similarity designed for sets of discrete objects. For two samples A and B, their OOC is calculated thus:

Equation 1.
$$OOC(A, B) = \frac{|A \cap B|}{\sqrt{|A| \times |B|}}$$

With the generalisation of molecular to joint assembly space, a corresponding Joint MA index can be calculated for a group of molecules. Joint MA index values lower than the sum of individual MAs indicate possible shared causal pathways among molecules in the group. Spurred by the Joint MA index's ability to capture the causal relationship between molecules, we proposed a further generalisation of this metric to tandem MS data of whole samples instead of individual molecules. The Joint Assembly Overlap (JAO) metric could serve as an indicator of hereditary connection between samples. We formulated JAO of sample A and B to lie between 0 and 1, 0 indicating no overlap and 1 full entailment, i.e. all molecules within one sample are contained within the joint assembly of the other. JAO is calculated thus:

Equation 2.
$$JAO(A, B) = \frac{JMA(A) + JMA(B)}{JMA(A + B)} - 1$$

with JMA standing for Joint MA.

Tree of life inference using the assembly metrics starts by calculating overlap values for each pair of samples, whether by fingerprinting, ACO or JAO. Following this initial calculation, an approximate iterative process is used, in which a matrix of scores amongst all samples is generated and the model clusters the samples that exhibit the highest similarity score. Using the Weighted Pair Group Method with Arithmetic Mean (WPGMA) algorithm, the matrix is then transformed to include the new clade containing the newly clustered samples by averaging their similarity scores to all the others groups in the matrix. This procedure is repeated until reaching a single root cladal group.

Biogenicity determination and cladal domain classification

We performed the classifications using either a supervised leave-one-out cross-validation method or an unsupervised spectral clustering method. In the first method, we iterated over the samples in the dataset, each time one sample was kept aside, and the rest were grouped according to their predefined real groups. We operated over the Fingerprinting, ACO and JAO matrices, where the prediction was made based on the maximal values for the examined kept-aside sample with other samples, assigning it to the group of its most-similar pair. For the second method of spectral clustering, we ran the algorithm on the numeric matrices, testing different numbers of clusters, using the *scikit* python package. We reported the Silhouette score for each number of clusters for each metric.

Structural elucidation of E. coli analytes

The MS² files were converted to abf files using AbfConverter (Reifycs). Samples were then checked and searched using MS Dial, an open-source software pipeline⁴³. Samples were searched against the NIST database in .msp format. Tolerances were set at 0.01 Da in the MS¹ and 0.05 Da in the MS². Retention time tolerance was 100 mins, and was not used for scoring or filtering. The matches were then crossed with known E. coli metabolites from a public repository⁴⁴. In addition, we extracted the SMILES of all metabolites in the repository and in-silico diffracted them using the CFM-IF4 docker software⁴⁵ to generate ESI MS/MS predicted spectra and compared them to the experimental spectra.

Matches were attained if a Jaccard similarity index between the lists of MS² peaks is above 0.1, and the difference between the masses is below two Daltons.

Statistical comparison between phylogenetic trees

We used the R packages TreeDist and Quartet to run the Generalized Robinson-Foulds (GRF) and Quartet similarity calculations, respectively. For the tree of life model, we defined four constraint states for the tree, and for each state generated 100,000 random trees whose randomness followed these constraints. T-tests were then conducted on each of the distributions, which were treated as the null-hypothesis for the assembly tree. For the recursive culturing experiment of *E. coli*, we generate the 135,135 possible tree constructs that consist of eight leaf nodes, and calculated their GRF and Quartet values to the experimental tree-like structure to anchor the values of the trees predicted by the phylogenetic models. We also conducted an exclusion assay, in which different permutations of samples are tested and the GRF and Quartet scores of the trees generated by the phylogenetic models using these samples are reported.

Data availability

All data used to for the analysis given in the SI and the figures will be available on publication.

Author Contributions

LC conceived the experimental framework building on the concept of the theory with help from SIW. AM developed the sample operating procedure, and AM and AK collected the mass spec data with input from EC. AK developed the data analysis approach building the tree of life and the classification methods, and did the statistical analyses. HM developed the Recursive MA algorithm and demonstrated its application to emulating JAS. MJ and AS helped develop the theoretical framework. LC and AK wrote the manuscript with input from all the authors.

Acknowledgements

We would like to thank Michael Lachmann (SFI) for comments on the manuscript, and Keith Patarroyo for his assistance in visualizing assembly pathways. We acknowledge financial support

from the John Templeton Foundation (grants 61184 and 62231), EPSRC (grant nos. EP/L023652/1, EP/R01308X/1, EP/S019472/1, and EP/P00153X/1), the Break-through Prize Foundation and NASA (Agnostic Biosignatures award no. 80NSSC18K1140), MINECO (project CTQ2017-87392-P), and ERC (project 670467 SMART-POM).

Conflict of Interest

A patent has been submitted on this work by the University of Glasgow, ref 2408156.4.

References

1. Mayr, E. *The Growth of Biological Thought: Diversity, Evolution, and Inheritance*. (Harvard University Press, 1982).
2. Linnaeus, C. *Systema Naturae per Regna Tria Naturae, Secundum Classes, Ordines, Genera, Species; Cum Characteribus, Differentiis, Synonymis, Locis*. vol. 1 (apud JB Delamolliere, 1789).
3. Darwin, C. & Bynum, W. F. *The Origin of Species by Means of Natural Selection: Or, the Preservation of Favored Races in the Struggle for Life*. (AL Burt New York, 2009).
4. Hug, L. A. *et al.* A new view of the tree of life. *Nat. Microbiol.* **1**, 1–6 (2016).
5. Delsuc, F., Brinkmann, H. & Philippe, H. Phylogenomics and the reconstruction of the tree of life. *Nat. Rev. Genet.* **6**, 361–375 (2005).
6. Mukherjee, S. *et al.* 1,003 reference genomes of bacterial and archaeal isolates expand coverage of the tree of life. *Nat. Biotechnol.* **35**, 676–683 (2017).
7. Parks, D. H. *et al.* A standardized bacterial taxonomy based on genome phylogeny substantially revises the tree of life. *Nat. Biotechnol.* **36**, 996–1004 (2018).
8. Ciccarelli, F. D. *et al.* Toward Automatic Reconstruction of a Highly Resolved Tree of Life. *Science* **311**, 1283–1287 (2006).
9. Gorbalenya, A. E. *et al.* The new scope of virus taxonomy: partitioning the virosphere into 15 hierarchical ranks. *Nat. Microbiol.* **5**, 668–674 (2020).
10. Mills, C. L., Beuning, P. J. & Ondrechen, M. J. Biochemical functional predictions for protein structures of unknown or uncertain function. *Comput. Struct. Biotechnol. J.* **13**, 182–191 (2015).

11. Parks, D. H. *et al.* Recovery of nearly 8,000 metagenome-assembled genomes substantially expands the tree of life. *Nat. Microbiol.* **2**, 1533–1542 (2017).
12. Kapli, P., Yang, Z. & Telford, M. J. Phylogenetic tree building in the genomic age. *Nat. Rev. Genet.* **21**, 428–444 (2020).
13. Muchowska, K. B., Varma, S. J. & Moran, J. Nonenzymatic Metabolic Reactions and Life's Origins. *Chem. Rev.* **120**, 7708–7744 (2020).
14. Lancet, D., Zidovetzki, R. & Markovitch, O. Systems protobiology: origin of life in lipid catalytic networks. *J. R. Soc. Interface* **15**, 20180159 (2018).
15. Bowman, J. C., Petrov, A. S., Frenkel-Pinter, M., Penev, P. I. & Williams, L. D. Root of the Tree: The Significance, Evolution, and Origins of the Ribosome. *Chem. Rev.* **120**, 4848–4878 (2020).
16. Singhal, N., Kumar, M., Kanaujia, P. K. & Viridi, J. S. MALDI-TOF mass spectrometry: an emerging technology for microbial identification and diagnosis. *Front. Microbiol.* **6**, (2015).
17. Sauer, S. & Kliem, M. Mass spectrometry tools for the classification and identification of bacteria. *Nat. Rev. Microbiol.* **8**, 74–82 (2010).
18. Lun, A. T. L., Swaminathan, K., Wong, J. W. H. & Downard, K. M. Mass Trees: A New Phylogenetic Approach and Algorithm to Chart Evolutionary History with Mass Spectrometry. *Anal. Chem.* **85**, 5475–5482 (2013).
19. Downard, K. M. Sequence-Free Phylogenetics with Mass Spectrometry. *Mass Spectrom. Rev.* **41**, 3–14 (2022).
20. Han, S. *et al.* A metabolomics pipeline for the mechanistic interrogation of the gut microbiome. *Nature* **595**, 415–420 (2021).
21. Sandrin, T. R., Goldstein, J. E. & Schumaker, S. MALDI TOF MS profiling of bacteria at the strain level: A review. *Mass Spectrom. Rev.* **32**, 188–217 (2013).
22. Musah, R. A. *et al.* A High Throughput Ambient Mass Spectrometric Approach to Species Identification and Classification from Chemical Fingerprint Signatures. *Sci. Rep.* **5**, 11520 (2015).
23. Chalupová, J., Raus, M., Sedlářová, M. & Šebela, M. Identification of fungal microorganisms by MALDI-TOF mass spectrometry. *Biotechnol. Adv.* **32**, 230–241 (2014).
24. Gregor, R. *et al.* Mammalian gut metabolomes mirror microbiome composition and host phylogeny. *ISME J.* **16**, 1262–1274 (2022).

25. Johnson, C. H., Ivanisevic, J. & Siuzdak, G. Metabolomics: beyond biomarkers and towards mechanisms. *Nat. Rev. Mol. Cell Biol.* **17**, 451–459 (2016).
26. D’Ari, R. & Casadesús, J. Underground metabolism. *BioEssays* **20**, 181–186 (1998).
27. Marshall, S. M. *et al.* Identifying molecules as biosignatures with assembly theory and mass spectrometry. *Nat. Commun.* **12**, 3033 (2021).
28. Jirasek, M. *et al.* Determining Molecular Complexity using Assembly Theory and Spectroscopy. Preprint at <https://doi.org/10.48550/arXiv.2302.13753> (2023).
29. Liu, Y. *et al.* Exploring and mapping chemical space with molecular assembly trees. *Sci. Adv.* **7**, eabj2465 (2021).
30. Sharma, A. *et al.* Assembly theory explains and quantifies selection and evolution. *Nature* 1–8 (2023).
31. Radoš, D., Donati, S., Lempp, M., Rapp, J. & Link, H. Homeostasis of the biosynthetic *E. coli* metabolome. *IScience* **25**, (2022).
32. Rosato, A. *et al.* From correlation to causation: analysis of metabolomics data using systems biology approaches. *Metabolomics* **14**, 1–20 (2018).
33. Borenstein, E., Kupiec, M., Feldman, M. W. & Ruppin, E. Large-scale reconstruction and phylogenetic analysis of metabolic environments. *Proc. Natl. Acad. Sci.* **105**, 14482–14487 (2008).
34. Reymond, J.-L., Ruddigkeit, L., Blum, L. & Deursen, R. van. The enumeration of chemical space. *WIREs Comput. Mol. Sci.* **2**, 717–733 (2012).
35. Verma, V. & Aggarwal, R. K. A comparative analysis of similarity measures akin to the Jaccard index in collaborative recommendations: empirical and theoretical perspective. *Soc. Netw. Anal. Min.* **10**, 43 (2020).
36. Kumar, S. *et al.* TimeTree 5: an expanded resource for species divergence times. *Mol. Biol. Evol.* **39**, msac174 (2022).
37. Smith, M. R. Information theoretic generalized Robinson–Foulds metrics for comparing phylogenetic trees. *Bioinformatics* **36**, 5007–5013 (2020).
38. Smith, M. R. Robust analysis of phylogenetic tree space. *Syst. Biol.* **71**, 1255–1270 (2022).
39. Broeckling, C. D., Hoyes, E., Richardson, K., Brown, J. M. & Prenni, J. E. Comprehensive Tandem-Mass-Spectrometry Coverage of Complex Samples Enabled by Data-Set-Dependent Acquisition. *Anal. Chem.* **90**, 8020–8027 (2018).

40. Koelmel, J. P. *et al.* Expanding Lipidome Coverage Using LC-MS/MS Data-Dependent Acquisition with Automated Exclusion List Generation. *J. Am. Soc. Mass Spectrom.* **28**, 908–917 (2017).
41. Davies, V. *et al.* Rapid Development of Improved Data-Dependent Acquisition Strategies. *Anal. Chem.* **93**, 5676–5683 (2021).
42. Cooper, B. & Yang, R. An assessment of AcquireX and Compound Discoverer software 3.3 for non-targeted metabolomics. *Sci. Rep.* **14**, 4841 (2024).
43. Tsugawa, H. *et al.* MS-DIAL: data-independent MS/MS deconvolution for comprehensive metabolome analysis. *Nat. Methods* **12**, 523–526 (2015).
44. Guo, A. C. *et al.* ECMDB: the E. coli Metabolome Database. *Nucleic Acids Res.* **41**, D625–D630 (2012).
45. Wang, F. *et al.* CFM-ID 4.0: More Accurate ESI-MS/MS Spectral Prediction and Compound Identification. *Anal. Chem.* **93**, 11692–11700 (2021).